comptes rendus palevol

2026 • 25 • 3

Virtual reconstruction and comparative study of the face of StW 573 (“Little Foot”)

Amélie BEAUDET, Emeline DUPONT, Franck GUY, Jean DUMONCEL, Robert ATWOOD, Vincent FERNANDEZ, Nghia T. VO, Ronald CLARKE, Jason L. HEATON, Travis R. PICKERING, Kristian J. CARLSON, Gérard SUBSOL & Dominic STRATFORD

LUCY’S HEIRS – TRIBUTE TO YVES COPPENS

Edited by Jean-Jacques HUBLIN, Aurélien MOUNIER & Nicolas TEYSSANDIER

art. 25 (3) — Published on 2 March 2026
www.cr-palevol.fr

PUBLICATIONS SCIENTIFIQUES

MUSÉUM NAL HIST NATURELLE

Couverture / *Cover* :
Made from the Figures of the article.

Comptes Rendus Palevol est indexé dans / Comptes Rendus Palevol *is indexed by:*
– Cambridge Scientific Abstracts
– Current Contents® Physical
– Chemical, and Earth Sciences®
– ISI Alerting Services®
– Geoabstracts, Geobase, Georef, Inspec, Pascal
– Science Citation Index®, Science Citation Index Expanded®
– Scopus®.

Les articles ainsi que les nouveautés nomenclaturales publiés dans *Comptes Rendus Palevol* sont référencés par / *Articles and nomenclatural novelties published in* Comptes Rendus Palevol *are registered on:*
– ZooBank® (http://zoobank.org)

Comptes Rendus Palevol est une revue en flux continu publiée par les Publications scientifiques du Muséum, Paris et l'Académie des sciences, Paris
Comptes Rendus Palevol *is a fast track journal published by the Museum Science Press, Paris and the Académie des sciences, Paris*

Les Publications scientifiques du Muséum publient aussi / *The Museum Science Press also publish:*
Adansonia, ***Geodiversitas***, ***Zoosystema***, ***Anthropozoologica***, ***European Journal of Taxonomy***, ***Naturae***, ***Cryptogamie*** **sous-sections** ***Algologie***, ***Bryologie***, ***Mycologie***.

L'Académie des sciences publie aussi / *The Académie des sciences also publishes:*
Comptes Rendus Mathématique, ***Comptes Rendus Physique***, ***Comptes Rendus Mécanique***, ***Comptes Rendus Chimie***, ***Comptes Rendus Géoscience***, ***Comptes Rendus Biologies***.

Diffusion – Publications scientifiques Muséum national d'Histoire naturelle
CP 41 – 57 rue Cuvier F-75231 Paris cedex 05 (France)
Tél. : 33 (0)1 40 79 48 05 / Fax : 33 (0)1 40 79 38 40
diff.pub@mnhn.fr / https://sciencepress.mnhn.fr

Académie des sciences, Institut de France, 23 quai de Conti, 75006 Paris.

ISSN (imprimé / *print*) : 1631-0683/ ISSN (électronique / *electronic*) : 1777-571X

Virtual reconstruction and comparative study of the face of StW 573 (“Little Foot”)

Amélie BEAUDET
Laboratoire de Paléontologie, Évolution, Paléoécosystèmes et Paléoprimatologie (PALEVOPRIM), CNRS, Université de Poitiers, 6 Rue Michel Brunet, F-86000 Poitiers (France)
and Department of Archaeology, University of Cambridge, Henry Wellcome Building, Fitzwilliam St, Cambridge CB2 1QH (United Kingdom)
and School of Geography, Archaeology and Environmental Studies, University of the Witwatersrand, Private Bag 3, WITS 2050 (South Africa)
amelie.beaudet@univ-poitiers.fr (corresponding author)

Emeline DUPONT
Franck GUY
Laboratoire de Paléontologie, Évolution, Paléoécosystèmes et Paléoprimatologie (PALEVOPRIM), CNRS, Université de Poitiers, 6 Rue Michel Brunet, F-86000 Poitiers (France)

Jean DUMONCEL
Centre de Recherches sur la Cognition et l’Apprentissage, CNRS, Université de Poitiers, Université de Tours, 5, rue T. Lefebvre, TSA 21103, F-86073 Poitiers Cedex 9 (France)

Robert ATWOOD
Diamond Light Source Ltd, Harwell Science and Innovation Campus, Didcot, Oxfordshire OX11 0DE (United Kingdom)

Vincent FERNANDEZ
Imaging and Analysis Centre, The Natural History Museum, Cromwell Road, South Kensington, London SW7 5BD (United Kingdom)
and European Synchrotron Radiation Facility, 71 rue des Martyrs, F-38000 Grenoble (France)

Nghia T. VO
Diamond Light Source Ltd, Harwell Science and Innovation Campus, Didcot, Oxfordshire OX11 0DE (United Kingdom)
and National Synchrotron Light Source II, Brookhaven National Laboratory, Upton, NY 11973 (United States)

Ronald CLARKE
Evolutionary Studies Institute, University of the Witwatersrand, Private Bag 3, WITS 2050 (South Africa)

Jason L. HEATON
Evolutionary Studies Institute, University of the Witwatersrand, Private Bag 3, WITS 2050 (South Africa)
and Department of Biology, University of Alabama at Birmingham, 464 Campbell Hall Birmingham, AL 35294-1170 (United States)

Travis R. PICKERING
Evolutionary Studies Institute, University of the Witwatersrand,
Private Bag 3, WITS 2050 (South Africa)
and Department of Anthropology, University of Wisconsin,
Madison, 1180 Observatory Dr #5240, Madison, WI 53706 (United States)

Kristian J. CARLSON
Evolutionary Studies Institute, University of the Witwatersrand,
Private Bag 3, WITS 2050 (South Africa)
and Division of Integrative Anatomical Sciences, Keck School of Medicine,
University of Southern California, 1333 San Pablo St. BMT 401
Los Angeles, CA 90033 (United States)

Gérard SUBSOL
Research-Team ICAR, Laboratoire d'Informatique, de Robotique
et de Microélectronique de Montpellier, CNRS, Université de Montpellier,
860 rue de St Priest, F-34095 Montpellier cedex 5 (France)

Dominic STRATFORD
School of Geography, Archaeology and Environmental Studies,
University of the Witwatersrand, Private Bag 3, WITS 2050 (South Africa)
and Department of Anthropology, Stony Brook University, Circle Rd,
SBS Building S-501, Stony Brook, NY 11794-4364 (United States)

Submitted on 18 February 2025 | Accepted on 2 October 2025 | Published on 2 March 2026

urn:lsid:zoobank.org:pub:B682CEB3-35B4-4427-8605-AE168C581BB3

Beaudet A., Dupont E., Guy F., Dumoncel J., Atwood R., Fernandez V., Vo N. T., Clarke R., Heaton J. L., Pickering T. R., Carlson K. J., Subsol G. & Stratford D. 2026. — Virtual reconstruction and comparative study of the face of StW 573 ("Little Foot"), *in* Hublin J.-J., Mounier A. & Teyssandier N. (eds), Lucy's Heirs – Tribute to Yves Coppens. *Comptes Rendus Palevol* 25 (3): 43-56. https://doi.org/10.5852/cr-palevol2026v25a3

ABSTRACT
Besides being taxonomically and phylogenetically informative, changes in the size and shape of the hominin face through time can reflect important functional adaptations. Recent discoveries of well-preserved *Australopithecus* crania, particularly StW 573 ("Little Foot") from Sterkfontein, South Africa, have enriched the fossil record. Although nearly complete, the StW 573 skull has suffered post-depositional damage, leading to the displacement and fragmentation of its facial structures. This study presents a preliminary digital reconstruction and comparative analyses of the StW 573 face. The skull was scanned at the Diamond Light Source (United Kingdom), and semi-automated segmentation was used to digitally separate bones and teeth from the surrounding matrix, and isolate bone fragments. The fragments were then digitally reassembled through visual alignment. The reconstructed StW 573 face was compared to those of *Gorilla*, *Homo*, *Pan*, and *Pongo*, and to the *Australopithecus* specimens Sts 5 (*Australopithecus africanus* from South Africa, 3.4-3.5 Ma) and A.L. 444-2 (*Australopithecus afarensis* from Ethiopia, 3.8 Ma), using standard linear measurements and a landmark-based geometric morphometric (GM) approach. The dimensions of the StW 573 reconstructed face, as assessed by the linear measurements, fall within the ranges observed in *Gorilla* and *Pongo*. Our GM analysis reveals that the shape of the reconstructed face of StW 573 is more similar to A.L. 444-2 than to Sts 5, with both fossils plotting close to extant *Pan* and *Pongo* groups in shape space. In addition to documenting close similarities between StW 573 and the eastern African *Australopithecus* specimen A.L. 444-2, our results provide new insights into the variability of the *Australopithecus* facial skeleton and raise questions on the adaptations and evolutionary polarity (e.g. ancestral pattern shared between eastern and southern African Pliocene *Australopithecus*) underlying changes affecting the orbital region within the genus.

KEY WORDS
Australopithecus, Sterkfontein, Pliocene hominins, synchrotron, geometric morphometrics.

RÉSUMÉ

Reconstruction virtuelle et étude comparative de la face de StW 573 (« Little Foot »).

En plus d'apporter des informations taxonomiques et phylogénétiques, les changements de la taille et la conformation de la face des hominines dans le temps sont susceptibles de refléter des adaptations fonctionnelles clés. Les découvertes récentes de crânes d'*Australopithecus* relativement bien préservés, en particulier celui de StW 573 (« Little Foot ») de Sterkfontein, Afrique du Sud, ont enrichi le registre fossile. Bien que presque complet, le crâne de StW 573 a subi des dommages post-dépositionnels, entrainant le déplacement et la fragmentation des structures de la face. Cette étude présente une reconstruction numérique ainsi que des analyses préliminaires de la face de StW 573. Le crâne a été scanné au Diamond Light Source (Royaume Uni), et une segmentation semi-automatisée a permis de séparer de façon numérique les os et dents de la matrice sédimentaire et d'isoler les os fragmentés. Ces fragments ont ensuite été réassemblés numériquement grâce à un processus d'alignement visuel. La face reconstruite de StW 573 a été comparée à celles de *Gorilla*, *Homo*, *Pan*, et *Pongo*, ainsi qu'aux spécimens d'*Australopithecus* Sts 5 (*Australopithecus africanus* d'Afrique du Sud, 3.4-3.5 Ma) et A.L. 444-2 (*Australopithecus afarensis* d'Ethiopie, 3.8 Ma), à partir de mesures linéaires standards et d'une approche de morphométrie géométrique (GM) par points repères. Les dimensions de la face reconstruite de StW 573, estimées à travers les mesures linéaires, tombent dans les variations observées pour *Gorilla* et *Pongo*. Notre analyse GM a révélé que la conformation de la face de StW 573 est plus proche de celle de A.L. 444-2 que de Sts 5, et que les deux fossiles sont proches des groupes actuels de *Pan* et *Pongo* dans l'espace de variation de la conformation. En plus de documenter des similitudes fortes entre StW 573 et le spécimen d'*Australopithecus* d'Afrique de l'Est A.L. 444-2, nos résultats fournissent de nouvelles données sur la variabilité de la face chez *Australopithecus* et posent des questions sur les adaptations et la polarité évolutionnaire (e.g. condition ancestrale partagée par *Australopithecus* en Afrique orientale et australe au Pliocène) sous-jacents aux changements qui ont affecté la région orbitaire au sein de ce genre.

MOTS CLÉS
Australopithecus, Sterkfontein, hominines du Pliocène, synchrotron, morphométrie géométrique.

INTRODUCTION

Changes in the shape and size of the face throughout the hominin lineage offer insights into key biological adaptations. The face, as a critical interface for the digestive, respiratory, visual, olfactory, non-verbal communication and vocalization systems, plays a significant role in mediating interactions between hominins and their physical and social environments (Aiello & Dean 2002; Lieberman 2011). While neutral evolutionary changes cannot be ruled out, it has been suggested that environmental factors influenced the evolution of hominin facial structures (Harvati & Weaver 2006). In particular, while random evolutionary processes may have been responsible for facial diversity within *Homo*, selection likely shaped the face of *Australopithecus* (Ackermann & Cheverud 2004; Schroeder *et al.* 2014), including relaxation of selection on masticatory force production (Ledogar *et al.* 2025). Accordingly, studying diachronic changes in the hominin face within a controlled geochronological context has the potential to reveal adaptive responses to environmental shifts that may have driven early hominin evolution (Bobe *et al.* 2002; Potts 2013; Sponheimer *et al.* 2013). Furthermore, comparative analysis of hominin facial anatomy has been instrumental in identifying diagnostic traits that distinguish hominin species and in clarifying phylogenetic relationships, especially among early hominins. For example, the presence of the anterior pillar has traditionally been used to identify southern African *Australopithecus* and *Paranthropus* specimens and to support the hypothesis of paraphyletic origins for eastern and southern African *Paranthropus* taxa since it is absent from eastern African forms (Rak 1983; but see Villmoare & Kimbel 2011).

Within the hominin lineage, the *Australopithecus* face differs significantly from that of both earlier (*Ardipithecus*) and later (*Homo*) hominin genera (reviewed in Lacruz *et al.* 2019). Diagnostic features of *Australopithecus* include a short and slightly prognathic maxilla, robust cranial superstructures, expansive zygomatic bones and flaring arches that connect the face and the braincase, small canines and incisors, and thick enamel (Rak 1983; Kimbel 2015). In contrast, *Ardipithecus ramidus* exhibits lightly built zygomatic bones, while the face of early *Homo* is more gracile, with the zygomatic bones facing laterally (Aiello & Dean 2002; Suwa *et al.* 2009). As a result, *Australopithecus* documents a pivotal stage in the evolutionary history of the hominin face, marked by changes implicating the size of the anterior teeth and the supraorbital regions and adaptations in the masticatory apparatus. Various factors have been proposed to account for these changes, including social interactions (e.g. reduced degree of sexual dimorphism) and dietary shifts (e.g. reduced mechanical demands of food mastication) (reviewed in Lockwood 1999; Lieberman 2011; Lacruz *et al.* 2019; Patterson *et al.* 2019; Ledogar *et al.* 2022).

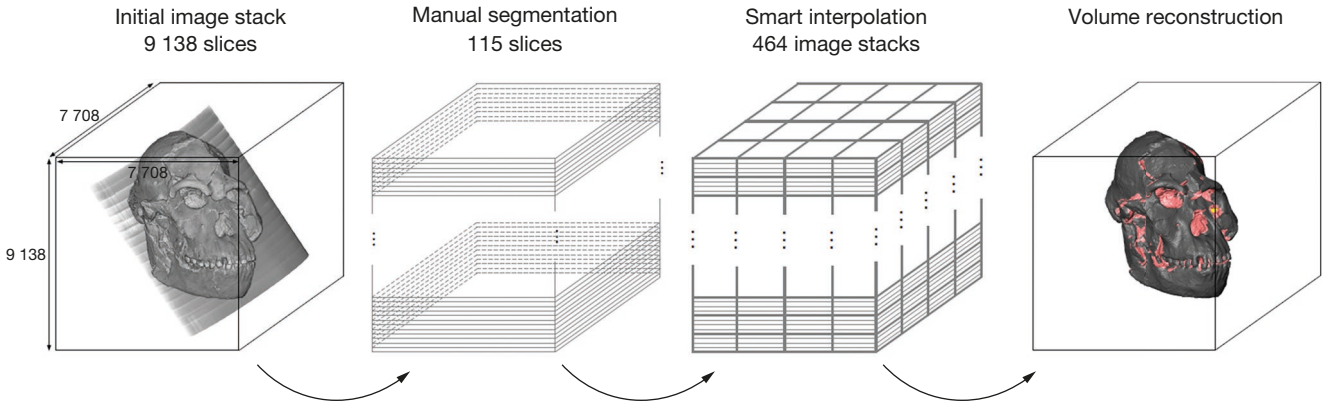

FIG. 1. — Semi-automated segmentation performed on the synchrotron-based images of the skull of StW 573. The skull and sediment are rendered in **grey** and **pink**, respectively. Credits: J. Dumoncel.

Investigating changes in the face of *Australopithecus* is not only valuable for understanding their interactions with social and physical environments, but also essential for documenting potential evolutionary trends and relationships among taxa. Currently, the origins of the taxic diversity within *Australopithecus* (with up to eight species described in the literature), the phylogenetic relationships among eastern, central and southern African taxa, and the role of the genus in the emergence of *Homo* remain subjects of debate (Wood *et al.* 2020; Reed *et al.* 2013; Alemseged 2023). Due to the abundance and morphology of their fossil remains, *Australopithecus afarensis* from eastern Africa and *Australopithecus africanus* from southern Africa have received considerable attention in discussion of the paleobiology of *Australopithecus* and the origins of *Homo*. However, for now, it is unclear how these two taxa, as well as the two species *Australopithecus anamensis* and *Australopithecus prometheus* that preceded and/or overlapped with them, might be related (Reed *et al.* 2013; Wood *et al.* 2020). Addressing this question is crucial for tracing the origins of *Australopithecus africanus*, and for identifying the evolutionary mechanisms (i.e., migration, isolation, speciation) that shaped the evolution of *Australopithecus* in Africa. In particular, morphological similarities between eastern and southern African *Australopithecus* specimens, as reported in the literature, may support a close phylogenetic relationship between these groups (Clarke & Kuman 2019), and could contribute to the discussion of possible migration patterns of *Australopithecus* between eastern and southern Africa (e.g. Alemseged 2023).

The *Australopithecus* record of southern Africa has been enriched by the discovery and description of well-preserved skulls, including MH1, attributed to *Australopithecus sediba* (De Ruiter *et al.* 2018), and StW 573 ("Little Foot"), a near-complete skeleton discovered in 1998 at Sterkfontein (South Africa), and fully excavated, cleaned and reconstructed by 2016 (Clarke 2019; Clarke & Kuman 2019). The nearly complete skull of StW 573, dated to *c.* 3.67 Ma (Granger *et al.* 2015) and assigned to *Australopithecus prometheus* (Clarke & Kuman 2019), has only minor bone loss in the basicranium. However, post-depositional damage has resulted in the lower face being displaced upward into the frontal and left zygomatic bones, while the frontal squama has been pushed downward. Additionally, the supraglabellar and temporal line regions on both sides are fragmented and buckled. Given that StW 573 is the oldest hominin in southern Africa, comparative study of the reconstructed face of StW 573 holds the potential to investigate morphological variation of the *Australopithecus* facial skeleton. Because our sample includes geologically younger specimens from eastern and southern Africa, such analyses offer the possibility to discuss evolutionary trends at a local (South Africa) and larger (continental) scale. Here, we present the first synchrotron-based digital reconstruction of the StW 573 skull along with preliminary results of the comparative analysis of the face and discuss how such results might support or challenge competing scenarios of the evolutionary history of the *Australopithecus* face.

MATERIAL AND METHODS

Comparative material

Our comparative sample of extant specimens includes non-pathological adult gorillas (*Gorilla gorilla*, N = 10), humans (*Homo sapiens*, N = 10), common chimpanzees (*Pan troglodytes*, N = 10), bonobos (*Pan paniscus*, N = 10), and orangutans (*Pongo pygmaeus*, N = 10) with equal proportions of females and males. Extant non-human specimens come from the British Museum (United Kingdom), the Museum of Comparative Zoology of Harvard University (United States), the Royal Museum for Central Africa in Tervuren (Belgium), the Staatssammlung für Anthropologie München (Germany) and the University of Zürich (Switzerland) (Neaux *et al.* 2013, 2015). The extant human individuals come from the Pretoria Bone Collection (PBC) of the University of Pretoria (South Africa, N = 8) and the British Museum (United Kingdom, N = 2). Ethical clearance for the use of extant human crania from the PBC was obtained from the Main Research Ethics committee of the Faculty of Health Sciences, University of Pretoria in February 2016 (ethics

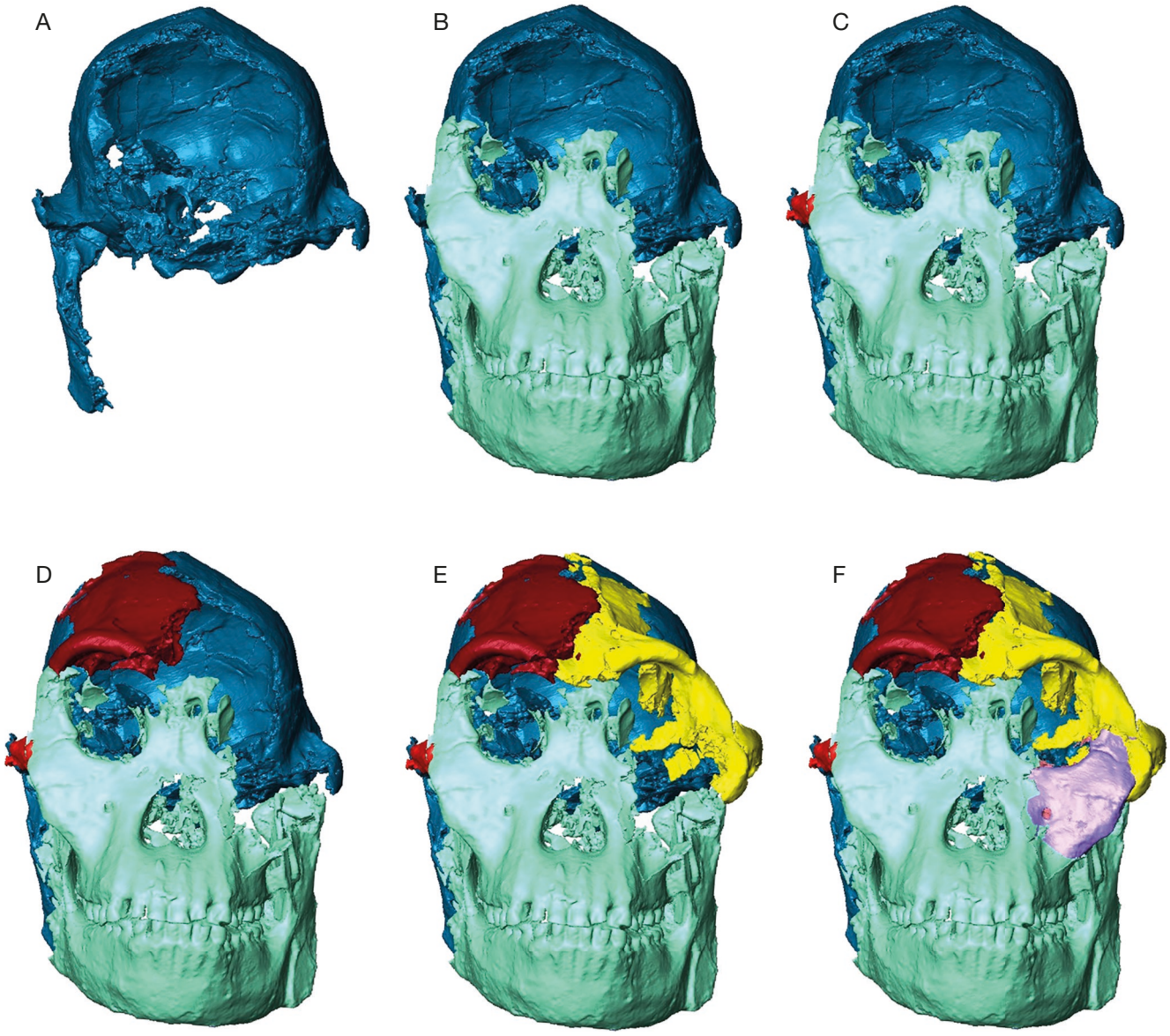

Fig. 2. — Reconstruction of the face of StW 573. The braincase and right ramus in **blue** (**A**) are aligned with the maxilla and the rest of the mandible in **green** (**B**). The portion of the right zygomatic arch in red is refitted to the temporal and zygomatic bones (**C**). The right frontal bone in dark red is positioned to fit with the maxilla (**D**). The left frontal bone and zygomatic in **yellow** (**E**) is repositioned to fit with the other blocks. The intact right maxilla is mirrored to reconstruct the left maxilla in **purple** (**F**). Credits: A. Beaudet.

reference 35/2016). In terms of comparative fossil specimens, we focused on the best preserved *Australopithecus* crania available, which include the *Australopithecus africanus* specimen Sts 5 from Sterkfontein Member 4 (South Africa), dated to 3.4-3.5 million years old (Granger *et al.* 2022), and the *Australopithecus afarensis* specimen A.L. 444-2 from Hadar (Ethiopia) dated to 3.18-2.94 million years old (Kimbel *et al.* 2004). Sts 5 and A.L. 444-2 are respectively housed in the Ditsong National Museum of Natural History (South Africa) and the Natural History Museum of Addis Ababa (Ethiopia). Additionally, we compared StW 573 with the published qualitative and quantitative description of the *Australopithecus anamensis* male specimen MRD-VP-1/1 from Woranso-Mille (Ethiopia) dated to 3.8 million years (Haile-Selassie *et al.* 2019).

Scanning and segmentation

The skull of StW 573 was scanned in 2019 by propagation phase-contrast synchrotron X-ray micro-computed tomography at the I12 beamline of the Diamond Light Source (United Kingdom) with an isotropic voxel size of 21.23 µm (see Beaudet *et al.* 2021 for further technical details). Extant comparative specimens were scanned by X-ray (micro)-tomography at the Center for Nanoscale Systems of Harvard University (United States), Department of Imaging & Pathology of the Katholieke Universiteit Leuven (Belgium), the Hammersmith Hospital (United Kingdom), the Kantonsspital Winterthur (Switzerland), a private radiology facility in Germany and the South African Nuclear Energy Corporation (South Africa) with a voxel size ranging from 0.1 to 1.0 mm. Sts 5 was scanned at the microfocus

TABLE 1. — Set of 34 landmarks positioned on the external surfaces of the faces of StW 573 and comparative samples (see Appendix 1). Fourteen of the landmarks were acquired bilaterally. Abbreviations: **L**, left; **R**, right.

Landmarks	Abbreviations	Number
Alare (R/L)	al	1
Alveolare I1/I2 (R/L)	aI1/I2	2
Alveolare C/P3 (R/L)	aC/P3	3
Alveolare P4/M1 (R/L)	aP4/M1	4
Alveolare M2/M3 (R/L)	aM2/M3	5
Frontomalare orbitale (R/L)	fmo	6
Frontomalare temporale (R/L)	fmt	7
Greater palatine foramen (R)	gpf	8
Incisive canal	inc	9
Infraorbital foramen (R/L)	inf	10
Lacrymale foramen (R/L)	lf	11
Nasospinale	ns	12
Orbitale (R/L)	or	13
Prosthion	pr	14
Rhinion	rhi	15
Staphylion	sta	16
Superior margin of the orbit (R/L)	smo	17
Lacrymale (R/L)	l	18
Zygoorbitale (R/L)	zyo	19
Zygomaxillare (R/L)	zm	20

TABLE 2. — Linear measurements assessed in StW 573 and the comparative sample. Distances are computed as inter-landmark distances. Abbreviations: **L**, left; **R**, right.

Measurements	Abbreviations	Distances
Biorbital breadth	FMOB	fmoR-fmoL
Upper facial breadth	UFB	fmtR-fmtL
Orbital height (R/L)	OBH	orR-smoR/orL-smoL
Orbital breadth (R/L)	OBB	fmoR-lR/fmoL-lL
Maxillo-alveolar breadth	MAB	aM2/M3R- aM2/M3L
Maxillo-alveolar length	MAL	pr-sta
Nasal breadth	NLB	alR-alL
Interorbital breadth	DKB	lR-lL
Lower face height	LFH	ns-pr

X-ray tomography facility of the Palaeosciences Centre at the University of the Witwatersrand (South Africa) at a voxel resolution of 0.075 mm. A.L. 444-2 was scanned using a medical scanner (computed tomography) with a pixel resolution of 0.41 mm and a slice thickness of 1 mm at the University Clinic in Innsbruck (Austria, Ledogar *et al.* 2022).

Semi-automated segmentation was applied to images of StW 573 to digitally separate bones and teeth from the matrix and isolate bone fragments using smart interpolation in Biomedisa (Lösel & Heuveline 2016; Lösel *et al.* 2020). Specifically, 115 slices (two successive slices being separated by 80 slices) were manually segmented using Avizo v2023.2 (FEI Visualization Sciences Group Inc., https://www.fei.com/software/amira-avizo/) out of the total 9 138 slices generated by the scanning process (Fig. 1). The smart interpolation tool of Biomedisa was applied to the resulting 464 image stacks, using the High-Performance Computing resources available at the Cambridge Service for Data-Driven Discovery (CSD3) of the University of Cambridge. Ultimately, the complete volume of StW 573 image data was reconstructed in 3D and additional manual cleaning was performed on Avizo v2023.2. 3D models of the extant comparative specimens and Sts 5 were generated using Avizo v2023.2 and 3D Slicer v5.2.2. (http://www.slicer.org, Fedorov *et al.* 2012). We used the reconstructed 3D model of A.L. 444-2 from the Virtual Anthropology repository of the University of Vienna (https://www.virtual-anthropology.com/download/al444-2_stl-format/#) (Ledogar *et al.* 2022).

Virtual reconstruction of StW 573

Based on the major displacements identified by Clarke & Kuman (2019), we identified five distinct blocks in the skull; the braincase attached to the right mandibular ramus (block 1), the maxilla and mandible (block 2), a portion of the right zygomatic arch (block 3), the right frontal bone (block 4), and the left frontal bone and zygomatic (block 5) (Fig. 2). All fragments were digitally positioned without adjusting for plastic deformation. As a result, in some cases (see Results), it was impossible to reposition the fragments into their correct anatomical alignment. We use block 1 as our starting point (Fig. 2A). Block 2 was slightly moved posteriorly to fit with block 1 (Fig. 2B). Block 3, which represents a portion of the right zygomatic arch, was refitted to other adjoining blocks (i.e., temporal and zygomatic bones of blocks 1 and 2, respectively) following anatomical correspondences. The lower face is considered as being relatively intact (Clarke & Kuman 2019). As such, the right frontal bone (block 4) was digitally positioned to fit with the zygomatic process, the frontal process and the orbital margin preserved in block 2 with a combination of translations and rotations (Fig. 2D). The left frontal bone and zygomatic (block 5) were similarly repositioned to fit with the other blocks (Fig. 2E). We mirrored the intact right maxilla to reconstruct the left side by ensuring that the mirrored surface fits the frontal process of block 2 and the zygomatic of block 5 (Fig. 2F). We manually removed portions of the mirrored surface that overlapped with existing surface of blocks 5 and 2. Permission to access and use the 3D surface of the reconstructed face of StW 573 can be granted by submitting a request to the curator of the Evolutionary Studies Institute (B. Zipfel) via MorphoSource (Sterkfontein project, https://www.morphosource.org/Detail/ProjectDetail/Show/project_id/632).

Linear measurements and shape analysis

A total of 34 landmarks were identified and positioned on the face of StW 573 and the comparative sample according to the landmark set traditionally used in the literature and the degree of preservation of StW 573 (i.e., we excluded any landmarks that could not be reliably identified due to taphonomic damage) (Table 1; Guy *et al.* 2005; Baab & McNulty 2009; Harvati & Hublin 2012; Neaux *et al.* 2013). Landmarks were positioned on the 3D models using the software 3D Slicer 5.2.2. (http://www.slicer.org, Fedorov *et al.* 2012). Based on landmark coordinates and distances, we assessed 9 linear measurements in StW 573 and the comparative extant and fossil samples (Table 2). Measurements were computed by using Euclidian distances. We included facial dimensions of MRD-VP-1/1 reported in Haile-Selassie *et al.* (2019) for comparative purposes.

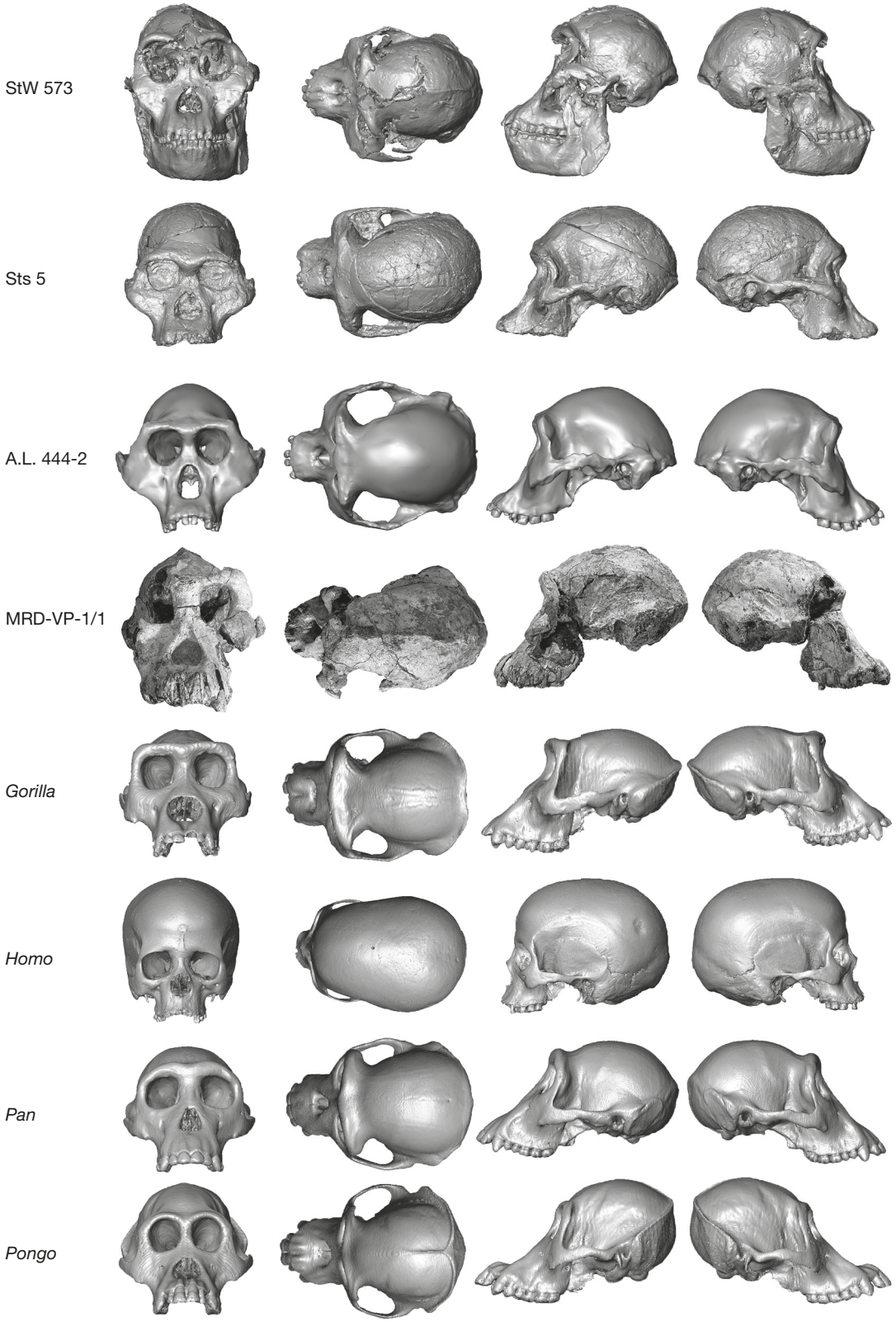

Fig. 3. — Comparison of the StW 573 cranium with the *Australopithecus africanus* specimen Sts 5, the *Australopithecus afarensis* specimen A.L. 444-2, the *Australopithecus anamensis* specimen MRD-VP-1/1 (courtesy of Y. Haile-Selassie) and extant *Gorilla*, *Homo*, *Pan* and *Pongo* specimens. From left to right, renderings are illustrated in anterior, superior, left lateral, and right lateral views. Images not to scale. Credits: A. Beaudet.

TABLE 3. — Linear measurements (in mm) of StW 573 and comparative fossil and extant material. See Table 2 for definitions and abbreviations. *, Measurements of MRD-VP-1/1 are from Haile-Selassie *et al.* (2019).

	FMOB	UFB	OBH-R	OBH-L	OBB-R	OBB-L	MAB	MAL	NLB	DKB	LFH
Fossil specimens											
StW 573	94.1	95.5	42.2	43.5	44.7	43.6	73.9	73.1	27.6	24.8	33.0
A.L. 444-2	93.2	117.9	41.1	41.1	39.4	39.8	66.5	77.7	27.9	18.2	28.2
MRD-VP-1/1	82.8*	98.5*	–	31.3*	–	31.5*	69.5*	–	24.1*	23.1*	30.7*
Sts 5	85.0	101.8	32.0	31.2	32.6	35.3	67.5	71.0	26.6	18.0	25.8
Extant taxa											
Gorilla gorilla											
mean	104.3	123.5	41.2	41.4	45.2	46.3	69.0	114.3	35.7	27.6	33.2
range	95.9-115.6	107.4-137.7	36.8-47.3	38.2-44.3	37.9-75.8	37.8-75.3	59.9-73.6	89.0-140.7	29.3-41.9	21.0-35.2	20.8-41.5
Homo sapiens											
mean	98.0	105.5	35.5	35.6	39.3	38.8	57.5	54.4	25.4	22.3	15.8
range	90.9-104.6	97.6-110.7	31.9-41.4	31.4-41.2	37.7-41.6	36.8-41.4	41.2-69.2	48.1-61.2	21.7-30.0	18.8-29.5	12.7-21.4
Pan paniscus											
mean	79.0	90.2	30.8	31.1	33.7	33.1	49.7	59.8	19.6	13.9	20.8
range	75.9-83.0	87.7-95.7	29.1-32.7	29.0-33.4	31.8-34.9	31.4-34.4	47.4-54.3	52.8-68.5	17.2-22.7	11.1-17.4	15.6-27.0
Pan troglodytes											
mean	86.2	99.7	33.0	33.2	34.4	34.8	57.7	75.1	24.0	19.2	28.1
range	79.5-90.8	92.8-109.7	30.1-35.4	30.1-36.4	32.5-37.1	33.0-36.9	52.0-62.3	68.7-84.4	20.5-27.9	13.6-23.7	20.0-37.0
Pongo pygmaeus											
mean	79.6	100.0	41.1	40.9	36.6	36.1	64.7	84.5	23.9	14.3	30.3
range	68.3-89.0	86.3-114.4	32.7-47.9	34.2-48.2	30.7-41.2	31.3-40.3	56.7-69.3	66.9-97.0	20.1-28.0	10.5-19.3	23.9-38.1

Shape of the StW 573 face was also quantitatively and comparatively investigated by applying a landmark-based 3D geometric morphometric approach. A generalized Procrustes analysis (Bookstein 1991) was computed on the coordinates of the set of 34 landmarks using RStudio 1.4.1106 (RStudio Team 2019) and the package "Morpho" (Schlager 2017). A principal component analysis (PCA) was performed to investigate shape variation within the comparative sample. Contributions of individual landmarks to total variance observed along each principal component (standardized loadings) were rendered by a color scale (Beaudet *et al.* 2016, 2019). The fossil specimens StW 573, Sts 5 and A.L. 444-2 were then projected onto the shape space defined by the extant taxa in the analysis.

RESULTS

Comparative description of the reconstructed face

Clarke & Kuman (2019) provided a detailed description of the skull of StW 573. In this paper we focus on a comparative description of the reconstructed face as represented in various anatomical views in Figure 3. The hexagonal facial mask as described in *Australopithecus* by Rak (1983) and Kimbel *et al.* (2004) is present in StW 573, but it is narrower as compared to those of Sts 5, A.L. 444-1 and MRD-VP-1/1 (figure 1 in Haile-Selassie *et al.* 2019), due to greater lateral expansion of the temporal process of zygomatic bones in the comparative specimens. The bone surface of the StW 573 midface is relatively flat, as in all *Australopithecus* specimens. Anterior pillars are present and laterally bordered by distinct grooves, as in Sts 5. The degree of prognathism in StW 573 is relatively high (about 80% when expressed as the percentage of palate length extending anterior to the coronal plane of sellion or as an index of prognathism, Rak 1983; Kimbel *et al.* 2004), particularly subnasally, as in MRD-VP-1/1. When considering the cranium in a lateral view, the deepest part of the face is located at the level of the nasal aperture, as in A.L. 444-2 (Kimbel *et al.* 2004).

Even though this part of the face is damaged, there is no visible supratoral sulcus, and separation of the supraorbital torus from the frontal squama is not as marked as it is in the comparative hominin crania. Consequently, the supraorbital region is not as projected anteriorly as in Sts 5 and, in superior view, it does not entirely cover the orbital region. The anterior root of the zygomatic approximates the level of the orbital floor in StW 573 and A.L. 444-2. Thickness of the right zygomatic arch is relatively constant, as in Sts 5, while it increases greatly from the posterior root to the anterior root in A.L. 444-2. The upper margin of the right arch forms a right angle with the frontal process of the zygomatic bone in StW 573, while it drops inferiorly in Sts 5 and A.L. 444-2. In superior view, the right zygomatic is arched as in A.L. 444-2, while that of Sts 5 is relatively straight. The frontal process in StW 573 resembles that of Sts 5 in facing forward and being sharply angulated, and the root is not as large as in A.L. 444-2 or MRD-VP-1/1. The zygomatic prominence in Sts 5 and other southern African *Australopithecus* crania (Kimbel *et al.* 2004) is absent in StW 573. In frontal view, the reconstructed right zygomaticoalveolar crest is straight in StW 573 resembling MRD-VP-1/1, but is not as curved as in Sts 5 and A.L. 444-2.

The interorbital region in StW 573 is wider than in A.L. 444-2 and is more similar to those in *Gorilla* and *Pan*. There is a distinct ridge running along the midline of the StW 573 nasals below the glabellar region that is absent in the comparative hominins, but that is present in *Gorilla*. As in A.L. 444-2, the nasoalveolar clivus forms a broad and convex arch in

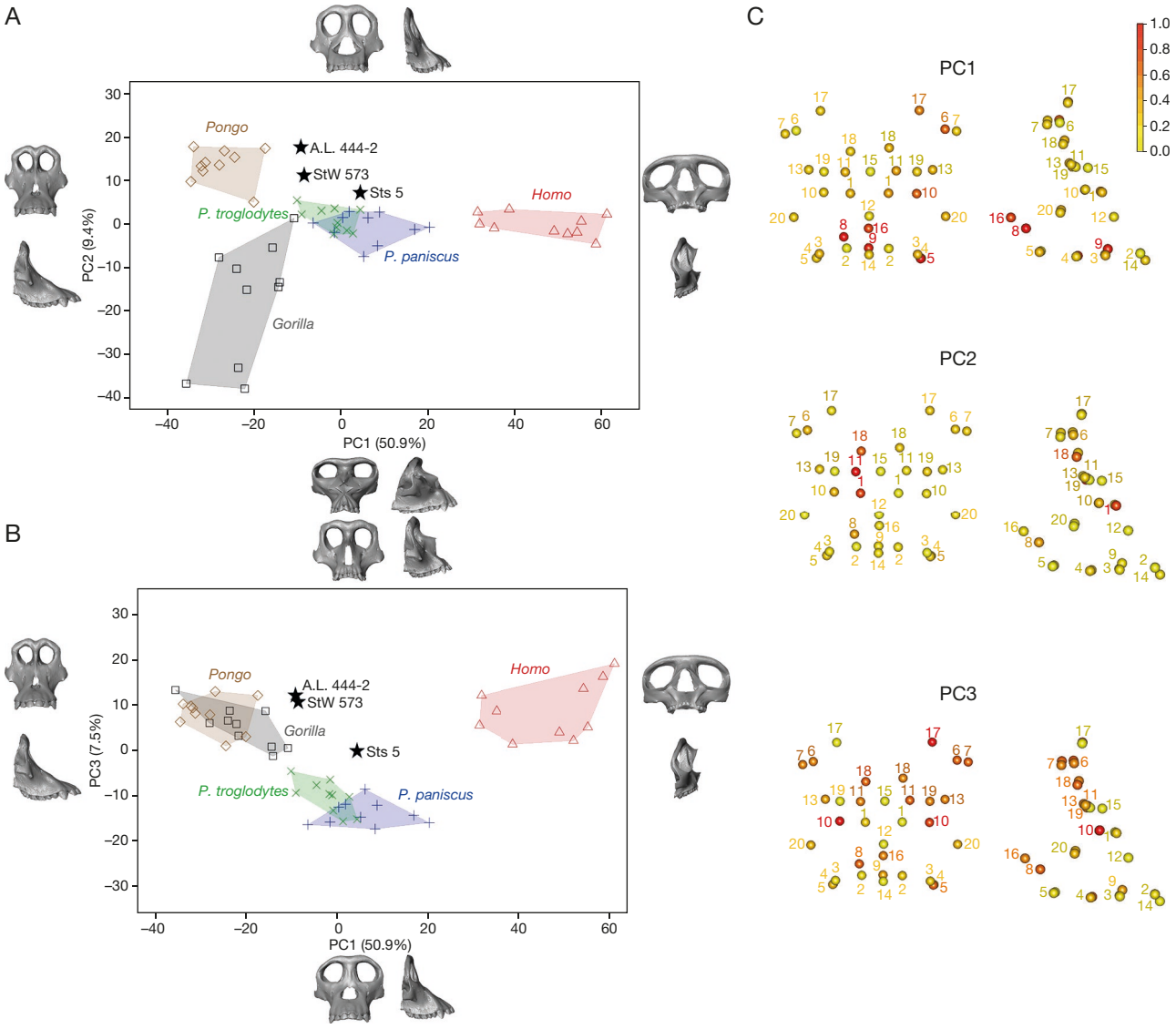

FIG. 4. — Principal component analysis of Procrustes-registered shape coordinates of facial morphology calculated for StW 573 and comparative samples for PC1, PC2 (**A**) and PC3 (**B**). Shapes at the extremes of the axes illustrate morphological variation trends along each principal component in anterior and lateral views. Contributions of landmarks to total variance along each principal component are rendered by a colour scale range from 0 (**yellow**) to 1 (**red**) (**C**). Credits: A. Beaudet.

StW 573 (Kimbel *et al.* 2004; Villmoare *et al.* 2014) that differs from the "nasoalveolar triangular frame" (Rak 1983) seen in Sts 5. The nasal bones of StW 573 widen inferiorly and are relatively flat, as in Sts 5. Due to the presence of anterior pillars in StW 573, lateral margins of the nasal aperture are smooth, as in Sts 5. The piriform aperture of StW 573 is not as tall as in A.L. 444-2, but it is broader, with a maximum width closer to the inferior margin, which means that the proportions of the triangle formed by the opening are more similar to those of Sts 5. Supraorbital tori and superior orbital margins of StW 573 are arched, as in Sts 5, *Pan* and *Pongo*, while the superolateral corners are not sharply angulated as in A.L. 444-2, MRD-VP-1/1 or *Gorilla*. The StW 573 orbits are tall and wide, and have an oval shape similar to the orbits of MRD-VP-1/1 (Haile-Selassie *et al.* 2019) and those of *Pongo*, and, to a lesser extent, those of A.L. 444-2. This shape differs from the rectangular orbits of Sts 5. The superior margin of the nasal aperture in StW 573 is located below the inferior orbital line, as in Sts 5, *Gorilla* and *Pongo*. The StW 573 aperture does not reach the level of the inferior margins of the orbits, as in A.L. 444-2 and *Homo*.

Linear measurements

Linear measurements are summarized in Table 3. Biorbital breadth of StW 573 is smaller than that of *Gorilla* but broader than those of *Pan* and *Pongo*, placing the former within the range of *Homo*. In contrast, upper facial breadth of StW 573 aligns with variation observed in *Pan* and *Pongo*. Orbit dimensions of StW 573 fall comfortably within *Gorilla* and *Pongo*. Maxillo-alveolar breadth of StW 573 is notably broad, exceeding all extant variation, but it remains relatively close to the upper end of the *Gorilla* range. Maxillo-alveolar length of StW 573 aligns with ranges in *Pan* and *Pongo*. Nasal breadth of StW 573 is comparable to those of *Homo*, *Pan*, and

Pongo, while interorbital breadth is more consistent with the variation seen in *Gorilla* and *Homo*. Lower face height closely approximates the mean of measurements for *Gorilla* and falls within the ranges of *Pan* and *Pongo*. Linear measurements in StW 573 are generally larger than those reported for Sts 5, except for upper facial breadth, and are more similar to those observed in A.L. 444-2 (e.g. biorbital breadth, orbital height and nasal breadth) or MRD-VP-1/1 (e.g. upper and lower face height and interorbital breadth).

Shape analysis

Figure 4 presents the PCA performed on Procrustes shape coordinates of the face. Along PC1, *Gorilla* and *Pongo* plot in the negative range. This corresponds to a more constricted upper face and interorbital distance, more rounded orbits, a narrower nasal aperture and an elongated maxilla. *Homo* occupies the space defined by positive values, which reflects a broader upper face and interorbital distance, wider orbits and nasal aperture, and a shorter maxilla. *Pan* plots between these two groups. PC2 roughly separates *Gorilla*, with its wide orbits, projecting midface and more constricted nasal aperture and lower face, from *Pongo*, with its taller orbits, flatter midface and broader nasal aperture. *Pan* and *Homo* occupy intermediate positions along this axis. PC3 primarily discriminates *Pan* (negative values), with its more rounded orbits and nasal aperture, flatter midface and a moderately long maxilla, from *Gorilla*, *Homo* and *Pongo*, with their taller orbits and nasal aperture, more elevated midface and shorter maxilla.

StW 573 and A.L. 444-2 plot closely along the three components. According to loadings, nearly all landmarks contribute to variance on PC1, with more substantial contributions of the landmarks placed on the palate. Along PC1, the three fossil specimens are situated near the *Pan* group, exhibiting an intermediate morphology between *Gorilla*/*Pongo* and *Homo* patterns. Variation along PC2 is primarily driven by differences in configurations of the nasal aperture and orbits, resulting in StW 573 and A.L. 444-2 more closely aligning with extant *Pongo*. Along PC3, StW 573 and A.L. 444-2 reside near *Pongo* and *Gorilla* groups. Warpings and loadings reveal that shape variation on PC3 predominantly implicates orbital regions, with affinities between the fossil specimens and *Pongo* and *Gorilla* reflecting similarities in their superior orbital margins and interorbital regions.

DISCUSSION

Our comparative and quantitative analysis of the StW 573 face highlights dimensional and morphological affinities with eastern African *Australopithecus* specimens and extant hominoids, as well as peculiar traits. In terms of overall size, StW 573 more closely approximates the dimensions of A.L. 444-2 and MRD-VP-1/1 than Sts 5, as well as those of extant *Gorilla*. General facial morphology, as represented by our landmark set, aligns StW 573 more closely with A.L. 444-2 than with Sts 5. In particular, dimensions and shape of the orbits resemble those of MRD-VP-1/1, A.L. 444-2 and *Pongo*. Finally, StW 573 also exhibits traits that were absent from comparative fossil specimens, such as the pinch along the midline of the nasals that may correspond to a greater reinforcement of the internasal suture.

While confirming an overall facial morphology in *Australopithecus* that shares similarities with that of *Pan*, our study highlights morphological differences between Sts 5 on the one hand and StW 573, A.L. 444-2 and MRD-VP-1/1 (to a lesser extent) on the other, particularly in the orbital region. Notably, previous similar morphometric approaches have also identified differences in craniofacial anatomy between Sts 5 and A.L. 444-2 (Guy *et al.* 2005), while Clarke & Kuman (2019)'s description of the StW 573 skull indicated affinities between "Little Foot" and eastern African *Australopithecus* specimens. Considering the geographical and temporal distributions of limited fossil specimens in the present study, our results support speculating that an overall "generalized" facial anatomy was possibly shared by StW 573 and MRD-VP-1/1, as previously noted for several features of the whole cranium by Clarke *et al.* (2021), and then persisted among eastern African *Australopithecus* groups, as reflected in the chronologically younger specimen A.L. 444-2. In contrast, if we consider the possibility that Sts 5 may be an accurate representation of the southern African *Australopithecus*, the hypothesis of the facial anatomy within southern African representatives of the genus becoming more "derived" than the eastern African forms might be examined (Rak 1983).

Regarding variation patterns in the facial anatomy of Pliocene hominins, our results indicate the presence of a distinct morphology in StW 573, particularly in the orbital region. Interestingly, orbital height varies independently of other facial characters and, therefore, has been suggested to represent a reliable diagnostic trait for distinguishing closely related primate taxa and evolutionary populations (Monson 2020). Additionally, variation in the size and orientation of primate orbits reveals functional (visual) and behavioral (ecological) adaptations (reviewed in Ankel-Simons & Rasmussen 2008; Heesy & Ross 2001; Heesy 2007). The morphology of StW 573 orbits, partly shared with eastern African *Australopithecus*, might therefore reveal useful information concerning visual capacities and ecological behavior of "Little Foot". In particular, even if the relationships between the orbital and visual cortex volume in primates can be debated (but see Pearce & Bridge 2013), our description of the endocast of "Little Foot" suggested an "ancestral" organization in the visual cortex, marked by an anteriorly placed lunate sulcus and, extended visual cortex (Beaudet *et al.* 2019). This configuration contrasts with a more "derived" position of the lunate sulcus found in the *Australopithecus* specimen StW 505 that derives from Sterkfontein Member 4, which also yielded Sts 5 (Holloway *et al.* 2004). Even though the mammalian skull is a highly integrated structure, previous studies have revealed the presence of a certain degree of modularity in the primate cranium, including within the face (Neaux *et al.* 2013; Esteve-Altava *et al.* 2015), that is responsible for mosaic-like evolution in the hominin head (reviewed in Lieberman 2011). Moreover, selective pressure

on the orbital region has been demonstrated to play a role in the diversification of early hominin faces (Ackermann & Cheverud 2004). Within this context, evolutionary pressure might have acted specifically on the orbital region in southern African Pliocene hominins, perhaps in conjunction with environmental instability leading to food resources becoming scarce and more difficult to spot or fallback foods requiring specific visual capacities (e.g. Joannes-Boyau *et al.* 2019).

However, several aspects have to be considered when interpreting the presented results in terms of phylogenetic affinities and function. In particular, sexual dimorphism is an additional factor to integrate when exploring interspecific variation within early hominins. Despite Lockwood *et al.* (1999) suggesting that *Australopithecus africanus* had a moderately high level of sexual dimorphism, intra-specific variation of facial traits described in this study, such as the orbits, is currently unknown within the southern African *Australopithecus* group. Additionally, taxic diversity is another factor to be considered since StW 573 was attributed by Clarke & Kuman (2019) to *Australopithecus prometheus*, thus differing from *Australopithecus africanus* (e.g. Sts 5) by a series of craniodental characters, including a robust zygomatic arch and broad interorbital distance. Finally, our reconstruction of StW 573 is preliminary and could likely be refined in the future, for example by using well-preserved contemporary hominin crania, such as MRD-VP-1/1, as references when validating our decisions regarding alignments and assembly of fragments. This step would be crucial to confirm specific traits preliminarily identified in StW 573, such as the absence of a clear separation between the face and neurocranium. Additionally, throughout the reconstruction process, we identified evidence of plastic deformation, in particular in the neurocranium, that will have to be corrected. Considering the geological context of Member 2 (Bruxelles *et al.* 2019), the most suitable approach to remove this deformation would be to model taphonomic processes, applying corrective retrodeformation and mechanical simulation to simulate forces acting on fossil remains during the fossilization process (Subsol *et al.* 2013).

Acknowledgements
We are indebted to G. Krüger and E. L'Abbé (Pretoria), L. Kgasi, H. Fourie and S. Potze (Pretoria), and S. Jirah and B. Zipfel (Johannesburg), and W. Wendelen (Tervuren) for having granted access to fossil and comparative material under their care. We also thank J. Hoffman and F. de Beer (Pelindaba), M. Dierick (Ghent) and R. Wuttge (Munich) for X-ray (micro)tomographic acquisitions. This work was carried out with the support of the Diamond Light Source, instrument I12 (experiment MG21334-1). We are grateful to the Ditsong National Museum of Natural History and the University of the Witwatersrand for loaning hominin crania in their collections. We thank the HEAS Virtual Anthropology Group for releasing 3D data of the *Australopithecus afarensis* cranium A.L. 444-2, and Y. Haile-Selassie for sharing photographs of MRD-VP-1/1. We are grateful to Lynn Copes, Lynn Lucas, and the MCZ for providing access to data originally appearing in Copes & Kimbel (2016) and Copes *et al.* (2016), the collection of which was funded by NSF DDIG #0925793, and a Wenner-Gren Foundation Dissertation Grant #8102 (both to Lynn Copes). Files were downloaded from https://www.MorphoSource.org, Duke University. For technical and/or scientific discussion/collaboration we are grateful to: M. Carmen Arriaza (Johannesburg), L. Bruxelles (Toulouse), R. Crompton (United Kindom), T. Jashashvili (United States), G. Krüger (Pretoria), K. Kuman (Johannesburg), A. Oettlé (Pretoria), M. Ponce de León (Zürich), J.F. Thackeray (Johannesburg) and C.P.E. Zollikofer (Zürich). We thank the DST-NRF for sponsoring the Micro-XCT facility at Necsa, and the DST-NRF and Wits University for funding the microfocus X-ray CT facility in the ESI (https://www.wits.ac.za/microct). Support of the Agence Nationale de la Recherche (ANR-24-CE02-2903), the Centre National de la Recherche Scientifique (CPJ-Hominines), the Claude Leon Foundation, the DST-NRF Center of Excellence in Palaeosciences (CoE-Pal),the French Institute of South Africa and the Diamond Light Source and the ISIS facility of the Science and Technology Facilities Council (STFC) towards this research is hereby acknowledged. Major funding for research, the Sterkfontein excavations and microCT scanning work have been provided by National Research Foundation grants to AB (#129336), KK (#82591 and 82611) and to DS (#98808) and by PAST. Opinions expressed and conclusions arrived at are those of the authors and are not necessarily to be attributed to the Center of Excellence in Palaeosciences. Ethical clearance for the use of extant human crania was obtained from the Main Research Ethics committee of the Faculty of Health Sciences, University of Pretoria in February 2016. We would like to thank the editor and the two anonymous reviewers for their time and effort in reviewing the manuscript, which greatly benefited from their comments.

REFERENCES

Ackermann R. R. & Cheverud J. M. 2004. — Detecting genetic drift versus selection in human evolution. *Proceedings of the National Academy of Sciences* 101 (52): 17946-17951. https://doi.org/10.1073/pnas.0405919102

Aiello L. & Dean C. (eds) 2002. — *An Introduction to Human Evolutionary Anatomy*. Academic Press, San Diego, 608 p. https://doi.org/10.1016/B978-0-08-057100-3.50028-6

Alemseged Z. 2023. — Reappraising the palaeobiology of *Australopithecus*. *Nature* 617: 45-54. https://doi.org/10.1038/s41586-023-05957-1

Ankel-Simons F. & Rasmussen D. T. 2008. — Diurnality, nocturnality, and the evolution of primate visual systems. *American Journal of Physical Anthropology* 137 S47 Supplement: Yearbook of Physical Anthropology: 100-117. https://doi.org/10.1002/ajpa.20957

Baab K. L. & McNulty K. P. 2009. — Size, shape, and asymmetry in fossil hominins: the status of the LB1 cranium based on 3D morphometric analyses. *Journal of Human Evolution* 57 (5): 608-622. https://doi.org/10.1016/j.jhevol.2008.08.011

Beaudet A., Dumoncel J., Thackeray J. F., Bruxelles L., Duployer B., Tenailleau C., Bam L., Hoffman J., De Beer F. & Braga J. 2016. — Upper third molar internal structural organization and semicircular canal morphology in Plio-Pleistocene South African cercopithecoids. *Journal of Human Evolution* 95: 104-120. https://doi.org/10.1016/j.jhevol.2016.04.004

Beaudet A., Clarke R. J., Bruxelles L., Carlson K. J., Crompton R., De Beer F., Dhaene J., Heaton J. L., Jakata K., Jashashvili T., Kuman K., McClymont J., Pickering T. R. & Stratford D. 2019. — The bony labyrinth of StW 573 ("Little Foot"): implications for early hominin evolution and paleobiology. *Journal of Human Evolution* 127: 67-80. https://doi.org/10.1016/j.jhevol.2018.12.002

Beaudet A., Atwood R. C., Kockelmann W., Fernandez V., Connolley T., Vo N. T., Clarke R. & Stratford D. 2021. — Preliminary paleohistological observations of the StW 573 ('Little Foot') skull. *eLife* 10: e64804. https://doi.org/10.7554/eLife.64804

Bobe R., Behrensmeyer A. K. & Chapman R. E. 2002. — Faunal change, environmental variability and late Pliocene hominin evolution. *Journal of Human Evolution* 42 (4): 475-497. https://doi.org/10.1006/jhev.2001.0535

Bookstein F. L. 1991. — *Morphometric Tools for Landmark Data: Geometry and Biology*. Cambridge University Press, Cambridge, 456 p. https://doi.org/10.1017/CBO9780511573064

Bruxelles L., Stratford D. J., Maire R., Pickering T. R., Heaton J. L., Beaudet A., Kuman K., Crompton R., Carlson K. J., Jashashvili T., Mcclymont J., Leader G. M. & Clarke R. J. 2019. — A multiscale stratigraphic investigation of the context of StW 573 'Little Foot' and Member 2, Sterkfontein Caves, South Africa. *Journal of Human Evolution* 133: 78-98. https://doi.org/10.1016/j.jhevol.2019.05.008

Clarke R. J. 2019. — Excavation, reconstruction and taphonomy of the StW 573 *Australopithecus prometheus* skeleton from Sterkfontein Caves, South Africa. *Journal of Human Evolution* 127: 41-53. https://doi.org/10.1016/j.jhevol.2018.11.010

Clarke R. J. & Kuman K. 2019. — The skull of StW 573, a 3.67 Ma *Australopithecus prometheus* skeleton from Sterkfontein Caves, South Africa. *Journal of Human Evolution* 134: 102634. https://doi.org/10.1016/j.jhevol.2019.06.005

Clarke R. J., Pickering T. R., Heaton J. L. & Kuman K. 2021 — The Earliest South African Hominids. *Annual Review of Anthropology* 50: 125-143. https://doi.org/10.1146/annurev-anthro-091619-124837

Copes L. E. & Kimbel W. H. 2016. — Cranial vault thickness in primates: *Homo erectus* does not have uniquely thick vault bones. *Journal of Human Evolution* 90: 120-34. https://doi.org/10.1016/j.jhevol.2015.08.008

Copes L. E., Lucas L. M., Thostenson J. O., Hoekstra H. E. & Boyer D. M. 2016. — A collection of non-human primate computed tomography scans housed in MorphoSource, a repository for 3D data. *Scientific Data* 3: 160001. https://doi.org/10.1038/sdata.2016.1

De Ruiter D. J., Carlson K. B., Brophy J. K., Churchill S. E., Carlson K. J. & Berger L. R. 2018 — The skull of *Australopithecus sediba*. *PaleoAnthropology* 2018: 56-155. https://doi.org/10.4207/PA.2018.ART112

Esteve-Altava B., Boughner J. C., Diogo R., Villmoare B. A. & Rasskin-Gutman D. 2015. — Anatomical network analysis shows decoupling of modular lability and complexity in the evolution of the primate skull. *PLOS ONE* 10: e0127653. https://doi.org/10.1371/journal.pone.0127653

Fedorov A., Beichel R., Kalpathy-Cramer J., Finet J., Fillion-Robin J.-C., Pujol S., Bauer C., Jennings D., Fennessy F., Sonka M., Buatti J., Aylward S., Miller J. V., Pieper S. & Kikinis R. 2012. — 3D Slicer as an image computing platform for the Quantitative Imaging Network. *Magnetic Resonance Imaging* 30: 1323-1341. https://doi.org/10.1016/j.mri.2012.05.001

Granger D., Gibbon R., Kuman K., Clarke R. J., Bruxelles L. & Caffee M. W. 2015. — New cosmogenic burial ages for Sterkfontein Member 2 *Australopithecus* and Member 5 Oldowan. *Nature* 522: 85-88. https://doi.org/10.1038/nature14268

Granger D. E., Stratford D., Bruxelles L., Gibbon R. J., Clarke R. J. & Kuman K. 2022. — Cosmogenic nuclide dating of Australopithecus at Sterkfontein, South Africa. *Proceedings of the National Academy of Sciences of the United States of America* 119 (27): e2123516119. https://doi.org/10.1073/pnas.2123516119

Guy F., Lieberman D. E., Pilbeam D., de León M. P., Likius A., Mackaye H. T., Vignaud P., Zollikofer C. & Brunet M. 2005. — Morphological affinities of the *Sahelanthropus tchadensis* (Late Miocene hominid from Chad) cranium. *Proceedings of the National Academy of Sciences* 102 (52): 18836-18841. https://doi.org/10.1073/pnas.0509564102

Haile-Selassie Y., Melillo S. M., Vazzana A., Benazzi S. & Ryan T. M. 2019. — A 3.8-million-year-old hominin cranium from Woranso-Mille, Ethiopia. *Nature* 573: 214-219. https://doi.org/10.1038/s41586-019-1513-8

Harvati K. & Hublin J.-J. 2012. — Morphological continuity of the face in the Late Middle and Late Pleistocene hominins from Northwestern Africa: a 3D geometric morphometric analysis, *in* Hublin J.-J. & McPherron S. P. (eds), *Modern Origins: A North African Perspective*. Springer Netherlands, Dordrecht: 179-188. https://doi.org/10.1007/978-94-007-2929-2_12

Harvati K. & Weaver T. D. 2006. — Human cranial anatomy and the differential preservation of population history and climate signatures. *The Anatomical Record Part A: Discoveries in Molecular, Cellular, and Evolutionary Biology* 288A (12): 1225-1233. https://doi.org/10.1002/ar.a.20395

Heesy C. P. 2007. — Ecomorphology of orbit orientation and the adaptive significance of binocular vision in primates and other mammals. *Brain Behavior and Evolution* 71 (1): 54-67. https://doi.org/10.1159/000108621

Heesy C. P. & Ross C. F. 2001. — Evolution of activity patterns and chromatic vision in primates: morphometrics, genetics and cladistics. *Journal of Human Evolution* 40 (2): 111-149. https://doi.org/10.1006/jhev.2000.0447

Holloway R. L., Clarke R. J. & Tobias P. V. 2004. — Posterior lunate sulcus in *Australopithecus africanus*: was Dart right? *Comptes Rendus Palevol* 3 (4): 287-293. https://doi.org/10.1016/j.crpv.2003.09.030

Joannes-Boyau R., Adams J. W., Austin C., Arora M., Moffat I., Herries A. I. R., Tonge M. P., Benazzi S., Evans A. R., Kullmer O., Wroe S., Dosseto A. & Fiorenza L. 2019. — Elemental signatures of *Australopithecus africanus* teeth reveal seasonal dietary stress. *Nature* 572: 112-115. https://doi.org/10.1038/s41586-019-1370-5

Kimbel W. H. 2015. —The species and diversity of australopiths, *in* Henke W. & Tattersall I. (eds), *Handbook of paleoanthropology*. Springer, New York: 2071-2106. https://doi.org/10.1007/978-3-642-39979-4_61

Kimbel W., Rak Y. & Johanson D. 2004. — The skull of *Australopithecus afarensis*. Oxford University Press, New York, 272 p. https://doi.org/10.1093/oso/9780195157062.001.0001

Lacruz R. S., Stringer C. B., Kimbel W. H., Wood B., Harvati K., O'higgins P., Bromage T. G. & Arsuaga J.-L. 2019. — The evolutionary history of the human face. *Nature Ecology & Evolution* 3: 726-736. https://doi.org/10.1038/s41559-019-0865-7

Ledogar J. A., Senck S., Villmoare B. A., Smith A. L., Weber G. W., Richmond B. G., Dechow P. C., Ross C. F., Grosse I. R., Wright B. W., Wang Q., Byron C., Benazzi S., Carlson K. J., Carlson K. B., Pryor Mcintosh L. C., Van Casteren A. & Strait D. S. 2022. — Mechanical compensation in the evolution of the early hominin feeding apparatus. *Proceedings of the Royal Society B: Biological Sciences* 289 (1977): 20220711. https://doi.org/10.1098/rspb.2022.0711

LEDOGAR J. A., BENAZZI S., SMITH A. L., DECHOW P. C., WANG Q., COOK R. W., NEAUX D., ROSS C. F., GROSSE I. R., WRIGHT B. W., WEBER G. W., BYRON C., WROE S. & STRAIT D. S. 2025 — Bite force production and the origin of *Homo*. *Royal Society Open Science* 12 (4): 241879. https://doi.org/10.1098/rsos.241879

LIEBERMAN D. E. 2011. — *The Evolution of the Human Head*. Harvard University Press, Cambridge, 768 p. https://doi.org/10.2307/j.ctvjnrtmh

LOCKWOOD C. A. 1999. — Sexual dimorphism in the face of *Australopithecus africanus*. *American Journal of Physical Anthropology* 108 (1): 97-127. https://doi.org/10.1002/(SICI)1096-8644(199901)108:1<97::AID-AJPA6>3.0.CO;2-O

LÖSEL P. & HEUVELINE V. 2016. — Enhancing a diffusion algorithm for 4D image segmentation using local information. *Proceedings of the Society of Photo-Optical Instrumentation Engineers* 9784: 97842L. https://doi.org/10.1117/12.2216202

LÖSEL P. D., VAN DE KAMP T., JAYME A., ERSHOV A., FARAGÓ T., PICHLER O., TAN JEROME N., AADEPU N., BREMER S., CHILINGARYAN S. A., HEETHOFF M., KOPMANN A., ODAR J., SCHMELZLE S., ZUBER M., WITTBRODT J., BAUMBACH T. & HEUVELINE V. 2020. — Introducing Biomedisa as an open-source online platform for biomedical image segmentation. *Nature Communications* 11: 5577. https://doi.org/10.1038/s41467-020-19303-w

MONSON T. A. 2020. — Patterns and magnitudes of craniofacial covariation in extant cercopithecids. *The Anatomical Record* 303 (12): 3068-3084. https://doi.org/10.1002/ar.24398

NEAUX D., GUY F., GILISSEN E., COUDYZER W., VIGNAUD P. & DUCROCQ S. 2013. — Facial orientation and facial shape in extant great apes: a geometric morphometric analysis of covariation. *PLOS ONE* 8: e57026. https://doi.org/10.1371/journal.pone.0057026

NEAUX D., GILISSEN E., COUDYZER W. & GUY F. 2015. — Integration between the face and the mandible of *Pongo* and the evolution of the craniofacial morphology of orangutans. *American Journal of Physical Anthropology* 158 (3): 475-486. https://doi.org/10.1002/ajpa.22807

PATTERSON D. B., BRAUN D. R., ALLEN K., BARR W. A., BEHRENSMEYER A. K., BIERNAT M., LEHMANN S. B., MADDOX T., MANTHI F. K., MERRITT S. R., MORRIS S. E., O'BRIEN K., REEVES J. S., WOOD B. A. & BOBE R. 2019. — Comparative isotopic evidence from East Turkana supports a dietary shift within the genus *Homo*. *Nature Ecology & Evolution* 3: 1048-1056. https://doi.org/10.1038/s41559-019-0916-0

PEARCE E. & BRIDGE H. 2013 — Is orbital volume associated with eyeball and visual cortex volume in humans? *Annals of Human Biology* 40 (6): 531-540. https://doi.org/10.3109/03014460.2013.815272

POTTS R. 2013. — Hominin evolution in settings of strong environmental variability. *Quaternary Science Reviews* 73: 1-13. https://doi.org/10.1016/j.quascirev.2013.04.003

RSTUDIO TEAM 2019. — *RStudio: Integrated Development for R*. RStudio, Inc., Boston, MA. http://www.rstudio.com/

RAK Y. 1983. — *The Australopithecine Face*. Academic Press, New York, 169 p.

REED K. E., FLEAGLE J. G. & LEAKEY R. E. 2013. — *The Paleobiology of* Australopithecus. Springer, Dordrecht, 282 p.

SCHLAGER S. 2017. — Chapter 9 - Morpho and Rvcg – Shape Analysis in R: R-Packages for Geometric Morphometrics, Shape Analysis and Surface Manipulations, *in* ZHENG G., LI S. & SZÉKELY G. (eds), *Statistical Shape and Deformation Analysis. Academic Press*: 217-256. https://doi.org/10.1016/B978-0-12-810493-4.00011-0

SCHROEDER L., ROSEMAN C. C., CHEVERUD J. M. & ACKERMANN R. R. 2014. — Characterizing the Evolutionary Path(s) to Early *Homo*. *PLOS ONE* 9 (12): e114307. https://doi.org/10.1371/journal.pone.0114307

SPONHEIMER M., ALEMSEGED Z., CERLING T. E., GRINE F. E., KIMBEL W. H., LEAKEY, M. G., LEE-THORP J. A., MANTHI F. K., REED K. E., WOOD B. A. & WYNN J. G. 2013. — Isotopic evidence of early hominin diets. *Proceedings of the National Academy of Sciences* 110 (26): 10513-10518. https://doi.org/10.1073/pnas.1222579110

SUBSOL G., CANU S., GILLES B., BRAGA J., COTIN S. & THACKERAY F. 2013. — 3D retrodeformation of paleoanthropological fossils based on biomechanical simulation. *American Journal of Physical Anthropology* S48: 266.

SUWA G., ASFAW B., KONO R. T., KUBO D., LOVEJOY C. O. & WHITE T. D. 2009. — The *Ardipithecus ramidus* skull and its implications for hominid origins. *Science* 326 (5949): 68-68e7. https://doi.org/10.1126/science.1175825

VILLMOARE B. A. & KIMBEL W. H. 2011. — CT-based study of internal structure of the anterior pillar in extinct hominins and its implications for the phylogeny of robust *Australopithecus*. *Proceedings of the National Academy of Sciences* 108 (39): 16200-16205. https://doi.org/10.1073/pnas.1105844108

VILLMOARE B. A., DUNMORE C., KILPATRICK S., OERTELT N., DEPEW M. J. & FISH J. L. 2014. — Craniofacial modularity, character analysis, and the evolution of the premaxilla in early African hominins. *Journal of Human Evolution* 77: 143-154. https://doi.org/10.1016/j.jhevol.2014.06.014

WOOD B., DOHERTY D. & BOYLE E. 2020. — Hominin Taxic Diversity. *Oxford Research Encyclopedia of Anthropology*. https://doi.org/10.1093/acrefore/9780190854584.013.194

Submitted on 18 February 2025;
accepted on 2 October 2025;
published on 2 March 2026.

APPENDIX

Appendix 1. — Set of landmarks positioned on the face of StW 573 in anterior (**A**) and inferior (**B**) views. Abbreviations: **aC/P3**, alveolare C/P3 (R/L); **al**, alare (R/L); **al1/l2**, alveolare I1/I2 (R/L); **aM2/aM3**, alveolare M2/M3 (R/L); **aP4/M1**, alveolare P4/M1 (R/L); **fmo**, frontomalare orbitale (R/L); **fmt**, frontomalare temporale (R/L); **gpf**, greater palatine foramen (R); **inc**, incisive canal; **inf**, infraorbital foramen (R/L); **l**, lacrymale (R/L); **lf**, lacrymale foramen (R/L); **ns**, nasospinale; **or**, orbitale (R/L); **pr**, prosthion; **rhi**, rhinion; **sta**, staphylion; **smo**, superior margin of the orbit (R/L); **zm**, zygomaxillare (R/L); **zyo**, zygoorbitale (R/L)